

# Application and modelling of ultrasonic transducers using 1-3 piezoelectric composites with structured electrodes

Dmitrij Dreiling<sup>1</sup>, Dominik Itner<sup>2</sup>, Nadine Feldmann<sup>1</sup>, Claus Scheidemann<sup>3</sup>, Hauke Gravenkamp<sup>4</sup>, Bernd Henning<sup>1</sup>

<sup>1</sup> Measurement Engineering Group, Paderborn University, 33098 Paderborn, Germany, Email: dreiling@emt.uni-paderborn.de

<sup>2</sup> Department of Civil Engineering, University of Duisburg-Essen, 45141 Essen, Germany

<sup>3</sup> Chair of Dynamics and Mechatronics, Paderborn University, 33098 Paderborn, Germany

<sup>4</sup> International Centre for Numerical Methods in Engineering (CIMNE), 08034 Barcelona, Spain

## Motivation

Waveguide-based methods can be used for the non-destructive determination of acoustic material parameters. One of these methods is based on transmission measurements of cylindrical polymeric samples. Here, the experimental setup consists of two transducers, which excite and receive the waveguide modes at the faces of the cylinder. 1-3 piezoelectric composites are used as an active element because of a dominant longitudinal excitation, which can be approximated as a pure thickness vibration. The measurement and a forward model are used to determine material parameters of the polymeric sample in an inverse approach. However, analyses show a low sensitivity in the determination of the mechanical shear parameter  $\mu_L$  due to the uniform excitation [1]. To increase the sensitivity of the transmission measurements to the shear parameter, segmented excitations shown exemplarily in Figure 1 were investigated by means of numerical simulations [2]. To realise the simulated ring- or sector-segmented excitation, new transducer prototypes are designed. As the inverse procedure for material parameter determination requires all parts of the measurement setup to be modelled, one-dimensional Mason models for the realised transducers are identified.

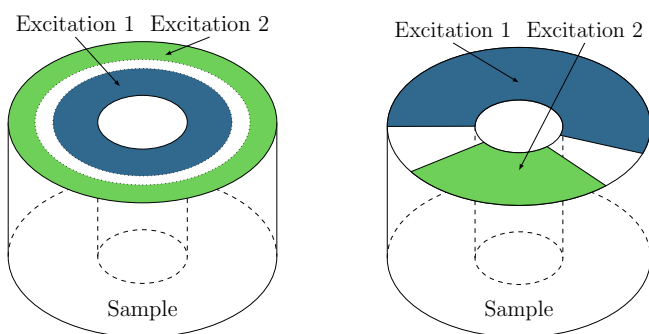


**Figure 1:** Segmented excitation with rings (left) and with sectors (right) to increase sensitivity with respect to shear parameter  $\mu_L$ .

## Structuring electrodes

To meet the assumptions of the sensitivity study [2], the segmented excitation needs to be purely normal to the specimens surface without any normal movement. The segmented excitation as shown in Figure 1 can be implemented by adapting the active element already in use.

Typically, 1-3 piezoelectric composites consist of piezoelectric rods embedded in a passive polymer matrix with electrodes on both faces (Figure 2). Due to the material

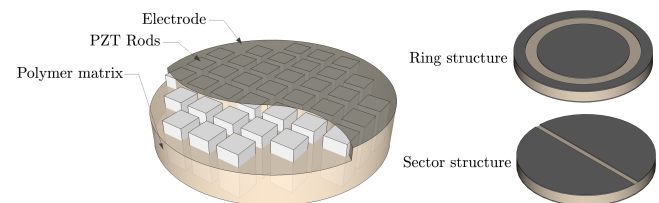


**Figure 2:** Schematic of a 1-3 piezoelectric composite disc and the two types of structured electrodes [3].

combination, the effective acoustic impedance of these piezocomposites is lower than that of comparable piezoceramics. In addition, the internal structure suppresses radial oscillations of the composite, resulting in dominant thickness oscillation. By subdividing the copper-tin (CuSn) electrodes of the composites via laser ablation, an electrical separation between the piezoelectric rods can be achieved. Measurements of the electrical impedance of two piezocomposites with a resonance frequency  $f_r \approx 1$  MHz shows the effects caused by the subdivision of the electrodes. Figure 3 shows the electrical impedance as a function of the frequency of a piezocomposite disc before and after subdividing one electrode into an inner and outer ring as well as a measurement of the impedance of another piezocomposite after subdividing the electrode in two halves (cf. Figure 2). The smaller area of the subdivided electrodes decreases the capacitance  $C_0^S$  of the piezocomposite disc and thus increases the overall absolute value of the impedance. Further, the mechanical quality factor  $Q_m$  of the thickness resonance at 1 MHz decreases. Because both halves have the same electrode area, there are only small differences between the impedances (Figure 3 below). The thickness resonance frequency still occurs close to 1 MHz regardless of the electrode subdivision, indicating the expected low coupling between thickness and radial modes.

## Modelling the piezoelectric composite

Because of the well-known dominant longitudinal excitation of 1-3 piezocomposites, a one-dimensional model is typically sufficient for an approximation of the electromechanical behaviour. Hence, a 3-port Mason model [4] is identified. This method of modelling is efficient com-

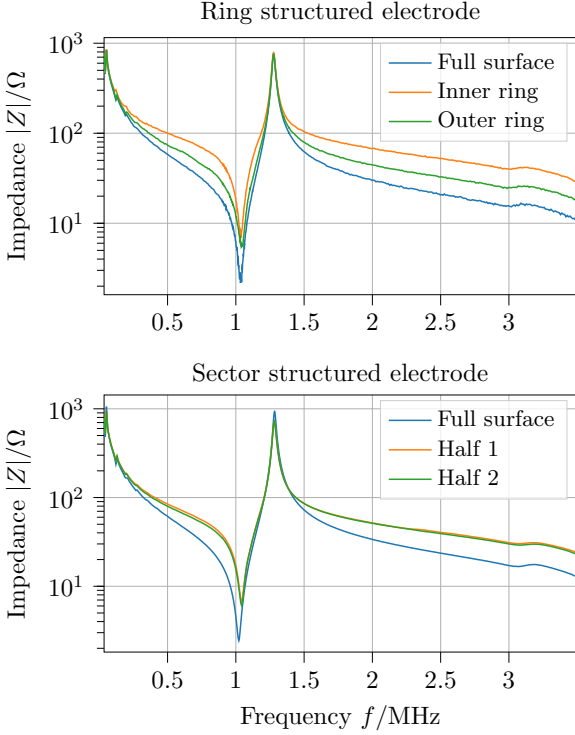


**Figure 3:** Impedance measurements of a composite before and after structuring the electrode.

pared to other modelling techniques, such as FEM simulations. Efficient modelling of the transducers is particularly necessary because the identified models are part of the forward model used in the inverse procedure, which is evaluated repeatedly during the optimisation process.

In the Mason model, the forces  $F_1, F_2$  applied on the composite and the resulting surface velocities  $v_1, v_2$  are related to the electrical voltage  $u$  and current  $i$  via a transfer matrix  $\mathbf{T}$ . With the composite thickness  $t_h$ , the transfer matrix  $\mathbf{T}$  can be described as:

$$\begin{bmatrix} F_1 \\ F_2 \\ u \end{bmatrix} = \mathbf{T} \cdot \begin{bmatrix} v_1 \\ v_2 \\ i \end{bmatrix}, \quad (1)$$

$$\mathbf{T} = \begin{bmatrix} Z_m \coth(\gamma t_h) & Z_m \operatorname{csch}(\gamma t_h) & h_{33}/(j\omega) \\ Z_m \operatorname{csch}(\gamma t_h) & Z_m \coth(\gamma t_h) & h_{33}/(j\omega) \\ h_{33}/(j\omega) & h_{33}/(j\omega) & 1/(j\omega C_0^S) \end{bmatrix}.$$

Here,  $Z_m, h_{33}, C_0^S$  and  $\gamma$  are the mechanical impedance, the piezoelectric coefficient in thickness direction, the clamped capacitance and the wave propagation constant, respectively. Moreover,  $\mathbf{T}$  depends on the angular frequency  $\omega$ . To account for losses, the model is extended using the mechanical quality factor  $Q_m$  [5, 6], resulting in the following definitions of the transfer matrix' parameters:

$$Z_m = \rho c_t^D A (1 + j 0.5 Q_m^{-1}), \quad h_{33} = c_t^D \sqrt{\frac{k_t^2 \rho}{\varepsilon_{33}^S}},$$

$$\gamma \approx \frac{\omega}{c_t^D} \frac{(0.5 Q_m^{-1} + j)}{\sqrt{(1 + 0.5 Q_m^{-2})}}, \quad C_0^S = \frac{\varepsilon_{33}^S A}{t_h}.$$

Assuming that the composite's area  $A$  can be determined by direct measurement, the parameter vector that needs to be identified is

$$\hat{\boldsymbol{\zeta}} = [\rho, c_t^D, k_t, Q_m, \varepsilon_{33}^S]^T, \quad (2)$$

with the density  $\rho$ , the speed of sound of the thickness mode  $c_t^D$ , the coupling factor  $k_t$ , the mechanical quality factor  $Q_m$ , and the electrical permittivity  $\varepsilon_{33}^S$ .

Assuming that both mechanical ports of the Mason model are terminated with the mechanical impedance of air ( $A \cdot 413.6 \text{ kg m}^{-2} \text{ s}^{-1}$ ), the system of equations constituted by Equation 1 can be rearranged to yield the electrical impedance  $|\hat{Z}(f, \hat{\boldsymbol{\zeta}})|$  of the model assuming free oscillation of the piezocomposite. This modelled impedance is matched to the measured electrical impedance of the actual sample using a local optimisation approach. Initial parameters  $\hat{\boldsymbol{\zeta}}_1$  can be determined using manufacturer information and analytical approximations [7]. As a target function for the optimisation, the logarithmic difference between measurement and simulation ( $\log_{10}(|Z(f)|) - \log_{10}(|\hat{Z}(f, \hat{\boldsymbol{\zeta}})|) = \log_{10}(|Z(f)|/|\hat{Z}(f, \hat{\boldsymbol{\zeta}})|)$ ) is used to account for the large range of the absolute value of the electrical impedance [8]. To further increase the optimisation process' robustness, a smooth approximation of the absolute value is used [9], yielding the full objective function:

$$S = \sum_{i=0}^N 2(\sqrt{1 + \log_{10}^2(|Z(f_i)|/|\hat{Z}(f_i, \hat{\boldsymbol{\zeta}})|)} - 1). \quad (3)$$

Because of cross-sensitivities, a multi-stage optimisation process at different frequency ranges applying the trust region reflective algorithm [9] is used, yielding the model parameters. The results for the Mason model with optimised parameters are shown in Figure 4 while Figure 5 shows the entire procedure in a schematic. Figure 4a shows the measured impedance of a raw piezocomposite with full-surface electrodes in comparison to the simulated impedance, showing good agreement in the considered frequency range. Figure 4b depicts the measured, frequency dependent impedance of the outer ring electrode as shown in Figure 2 and the impedance of the model. The same algorithm with adjusted initial model parameters  $\hat{\boldsymbol{\zeta}}_1$  is used to simulate the piezocomposites with structured electrodes. The adjustment includes the smaller piezocomposite area of excitation  $A$  and the associated reduction of the capacitance  $C_0^S$ . Further, the remaining model parameters from the optimised model parameters of the piezocomposite with full-surface electrodes are used. Figure 4c shows the measured and simulated impedance as a function of the frequency of the piezoelectric composite with an electrode structured in two sectors, again showing good agreement. It is evident that the Mason model is suitable for modelling the active element in the desired frequency range with structured electrodes.

## Transducer design

The schematic of the realised transducer is shown in Figure 6. It is based on a design developed by Rautenberg [6]

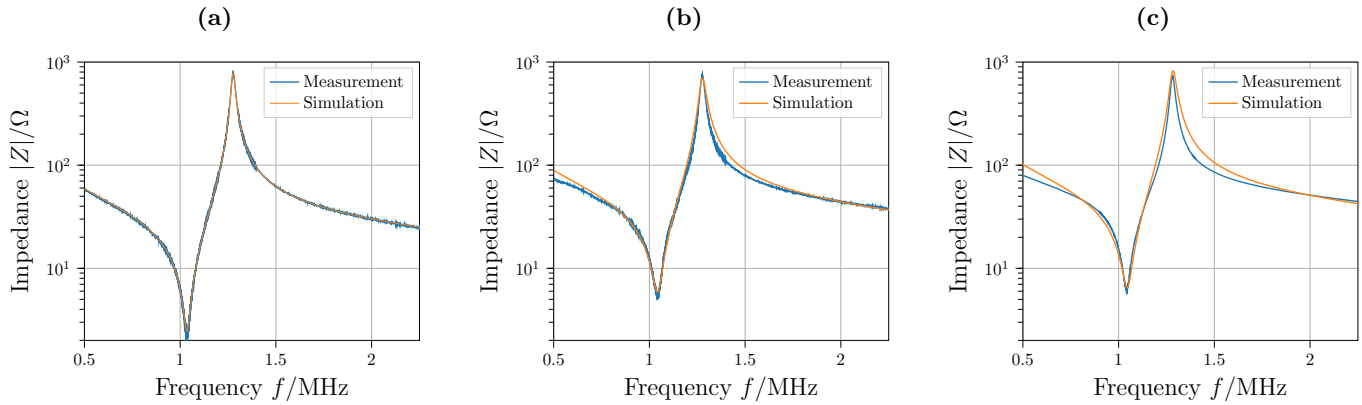


**Figure 4:** Comparison of the measured and simulated impedance of a composite with full-surface electrodes (a), outer ring electrode (b) and one sector electrode (c).

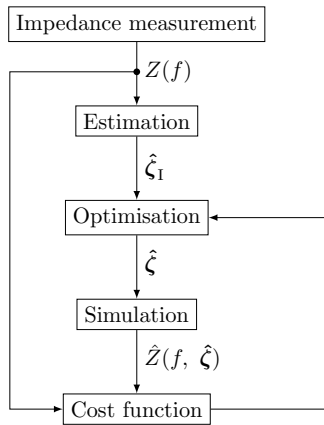


**Figure 5:** Schematic of the identification process parameters of the Mason model.

and Bause [1] that is extended to allow an active element with segmented electrodes. To protect the active element from mechanical damage, the 1-3 piezocomposite is adhesively fixed on a protective layer made of stainless steel (18Cr9Ni) with a thickness of 75  $\mu\text{m}$ . The protective layer is also used to electrically contact the lower electrode of the piezocomposite. To ensure the electric contact, the adhesive (Loctite EA9483) used is mixed with a small amount of silver powder. To supply signals to the

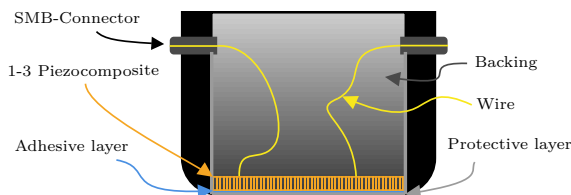


**Figure 6:** The design of a transducer with 1-3 piezocomposite with two structured electrodes.

transducer, SMB connectors are mounted on the sides of the transducers housing and electrically connected to the electrodes of the piezocomposite via thin copper wires. In the final step, the transducer is filled with a mixture of polyurethane and tungsten carbide powder for damping purposes. The mass mixing ratio is chosen to increase the

acoustic impedance as far as possible while avoiding inhomogeneities in the mixture (approximately 1 : 4.5) [3]. To describe the behaviour of the entire transducer, the 3-port Mason model is expanded by adding passive 2-ports for the adjacent layers Figure 8 [1]. The electrical network can be a matching network e.g. a  $\Pi$ -network or, in the simplest case, a model of the connected transmission line with the transfer matrix  $\mathbf{T}_{\text{el}}$ . In the case of a coaxial cable, the following equation applies for  $\mathbf{T}_{\text{el}}$  [5]:

$$\begin{bmatrix} u_2 \\ i_2 \end{bmatrix} = \begin{bmatrix} \cosh(\gamma l) & Z_w \sinh(\gamma l) \\ Z_w^{-1} \sinh(\gamma l) & \cosh(\gamma l) \end{bmatrix} \cdot \begin{bmatrix} u_1 \\ -i_1 \end{bmatrix}, \quad (4)$$

with the characteristic impedance  $Z_w$  and length  $l$  of the coaxial cable. Mechanical 2-ports are used to describe the adhesive and the protective layers. The transfer matrix  $\mathbf{T}_{\text{ac}}$  of such a layer is given as follows [5]:

$$\begin{bmatrix} \sigma_2 \\ v_2 \end{bmatrix} = \begin{bmatrix} \cosh(\gamma t_{\text{ac}}) & Z_{\text{ac}} \sinh(\gamma t_{\text{ac}}) \\ Z_{\text{ac}}^{-1} \sinh(\gamma t_{\text{ac}}) & \cosh(\gamma t_{\text{ac}}) \end{bmatrix} \cdot \begin{bmatrix} \sigma_1 \\ -v_1 \end{bmatrix}. \quad (5)$$

Here,  $Z_{\text{ac}}$  and  $t_{\text{ac}}$  are the acoustic impedance and thickness of each layer. The backing is included in the calculation as an acoustic impedance  $Z_{\text{B}}$  on one mechanical port of the 3-port Mason model. Due to the later coupling of the transducer model to a polymer sample, a transition of forces  $F_1, F_2$  to mechanical stresses  $\sigma_1, \sigma_2$  or the acoustic dynamic pressure is required. Utilising the chain matrix formulation, the electrical input and mechanical output of the transducer model can be described as follows:

$$\begin{bmatrix} \sigma_{\text{out}} \\ v_{\text{out}} \end{bmatrix} = \mathbf{T}_{\text{ac}}^{-1} \cdot \mathbf{T}_{\text{tr}} \cdot \mathbf{T} \cdot \mathbf{T}_{\text{el}}^{-1} \begin{bmatrix} u_{\text{in}} \\ -i_{\text{in}} \end{bmatrix}. \quad (6)$$

For the derivation of this transformation matrix  $\mathbf{T}_{\text{tr}}$ , refer to Bause [1]. The parameters of all transfer matrices (Equation 6) are again identified by optimisation using the approach presented in the previous section.

## Evaluation

Figures 7a and 7b show a comparison of the simulated impedance of the full transducer model as presented in Figure 8 with the electrical impedance of the physical transducer. Both results show good agreement between measurement and simulation, with larger deviations occurring where the transducer's electrode is segmented in

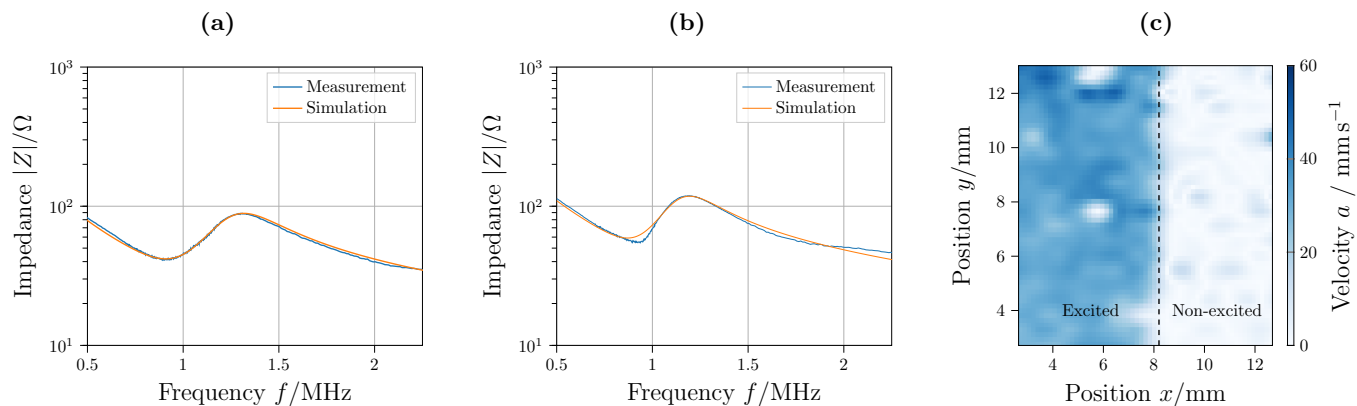


**Figure 7:** Comparison of the measured and simulated impedance of a transducer with ring electrode structure (a) and sector electrode structure (b). Surface velocity measurement of a transducer with structured electrodes (c).

two halves. This behaviour may be caused by the disrupted rotational symmetry. To further evaluate the electromechanical properties of the transducer, vibrometric surface velocity measurements are conducted. The results of a transducer with structured electrodes are shown in Figure 7c. A burst excitation at 1 MHz and 30 V amplitude is applied to the electrode covering the left side of the figure. As is clearly visible, only the left side shows oscillation with a maximum velocity of about  $50 \text{ mm s}^{-1}$ . Especially the transition region between the excited and non-excited electrode is sufficiently small for the assembled transducer, allowing for a highly selective excitation of different regions on the sample's surface required for future research.

### Summary

Using piezoelectric composites with electrodes structured by laser ablation, the authors show that transducers for spatially selective excitation of ultrasonic waves can be realised. These transducers can be modelled in an efficient, simplified manner using a 3-port Mason model along with 2-ports for the electrical and mechanical transmission lines. Surface velocity measurements show a good separation of excited and non-excited regions.

The realised transducers are to be used in material characterisation methods with increased sensitivity for shear parameters. Further research will include evaluations of thinner composites resulting in transducers with higher resonance frequency for the determination of frequency-dependent absorption behaviour.

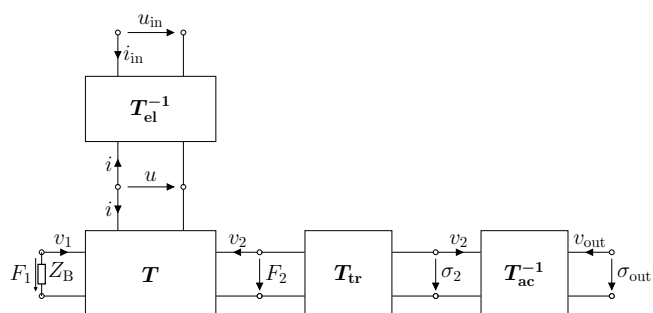


**Figure 8:** Full model of a transducer.

### Funding

The authors would like to thank the German Research Foundation (DFG, Deutsche Forschungsgemeinschaft) for financial support of the research project 409779252.

### References

- [1] Bause, F.: Ein ultraschallbasiertes inverses Messverfahren zur Charakterisierung viskoelastischer Materialparameter von Polymeren, PhD thesis, Paderborn University, 2016
- [2] Dreiling, D., Itner, D.T., Feldmann, N., Gravenkamp, H. and Henning, B.: Increasing the sensitivity in the determination of material parameters by using arbitrary loads in ultrasonic transmission measurements, SMSI 2020 Conference (2020), 261–262
- [3] Bause, F., Rautenberg, J., Henning, B.: Design, modeling and identification of an ultrasonic composite transducer for target impedance independent short pulse generation, AMA Conferences (2013), 68–73
- [4] Mason, W. P.: Electro-mechanical transducers and wave filters, van Nostrand, Princeton, 1948
- [5] Lerch, R., Sessler, G. and Wolf, D.: Technische Akustik – Grundlagen und Anwendungen, Springer, Heidelberg, Berlin, 2009
- [6] Rautenberg, J.: Ein wellenleiterbasiertes Verfahren zur Bestimmung von Materialdaten für die realitätsnahe Simulation von Schallausbreitungsphänomenen am Beispiel starkabsorbierender Kunststoffe, PhD thesis, Paderborn University, 2012
- [7] IEEE Standard on Piezoelectricity, 1987
- [8] Feldmann, N., Schulze, V., Claes, L., Jurgelucks, B., Walther, A., and Henning, B.: Inverse piezoelectric material parameter characterization using a single disc-shaped specimen, tm - Technisches Messen (2020), 50–55
- [9] Virtanen, P. et al.: SciPy 1.0: Fundamental Algorithms for Scientific Computing in Python, Nature Methods 17 (2020), 261–272